

INVERSE COMPTON SCATTERING MODEL FOR X-RAY EMISSION OF THE GAMMA-RAY BINARY LS 5039

M. S. Yamaguchi and F. Takahara

Department of Earth and Space Science, Graduate School of Science, Osaka University,
Toyonaka, Osaka, 560-0043, Japan

Received _____; accepted _____

ABSTRACT

We propose a model for the gamma-ray binary LS 5039 in which the X-ray emission is due to the inverse Compton (IC) process instead of the synchrotron radiation. Although the synchrotron model has been discussed in previous studies, it requires a strong magnetic field which leads to a severe suppression of the TeV gamma-ray flux in conflict with H.E.S.S. observations. In this paper, we calculate the IC emission by low energy electrons ($\gamma_e \lesssim 10^3$) in the Thomson regime. We find that IC emission of the low energy electrons can explain the X-ray flux and spectrum observed with *Suzaku* if the minimum Lorentz factor of injected electrons γ_{\min} is around 10^3 . In addition, we show that the *Suzaku* light curve is well reproduced if γ_{\min} varies in proportion to the *Fermi* flux when the distribution function of injected electrons at higher energies is fixed. We conclude that the emission from LS 5039 is well explained by the model with the IC emission from electrons whose injection properties are dependent on the orbital phase. Since the X-ray flux is primarily determined by the total number of cooling electrons, this conclusion is rather robust, although some mismatches between the model and observations at the GeV band remain in the present formulation.

Subject headings: binaries: close - radiation mechanisms: non-thermal - stars:
individual (LS5039) - X-rays: binaries

1. Introduction

Five gamma-ray binaries have been identified so far. They are LS 5039 (Aharonian et al. 2005a), LSI +61° 303 (Albert et al. 2006), PSR B1259-63 (Aharonian et al. 2005b), HESS J0632+057 (Aharonian et al. 2007; Bongiorno et al. 2011), and 1FGL J1018.6-5856 (Fermi LAT Collaboration et al. 2012). These systems consist of a compact object, a neutron star or a black hole, and an OB star (LS 5039 and 1FGL J1018.6-5856 have an O star while the others have a Be star). The nature of the compact objects is still open except for PSR B1259-63 whose primary star is known to be a young pulsar.

LS 5039 consists of a compact object and a massive star whose spectral type is O6.5 V and whose mass is $M_* = 22.9_{-2.9}^{+3.4} M_\odot$, and its binary period is 3.906 days (Casares et al. 2005). In addition, the system has the eccentricity, $e = 0.24 \pm 0.08$ (Sarty et al. 2011), and its separation changes from $\sim 2.6 R_*$ at periastron to $\sim 4.2 R_*$ at apastron, where $R_* = 9.3_{-0.6}^{+0.7} R_\odot$ represents the radius of the companion O star (Casares et al. 2005). Spectra and light curves of LS 5039 have been reported in the energy band of TeV gamma ray, GeV gamma ray, and X-ray, with H.E.S.S. array of atmospheric Cherenkov telescopes (Aharonian et al. 2006), *Fermi Gamma-ray Space Telescope* (Abdo et al. 2009), and *Suzaku* (Takahashi et al. 2009), respectively. These observations show that the fluxes clearly modulate with its binary period, which implies that the high energy emissions are generated within the system. In addition, we can see from the observational data that the X-ray flux anti-correlates with the GeV gamma-ray flux and correlates with the TeV flux. We note further that the photon index in the X-ray band is ~ 1.5 , which means that spectra of the electrons emitting X-rays have a power-law index ~ 2.0 .

Many authors have discussed the X-ray emission mechanism in LS 5039 assuming that it is due to the synchrotron radiation (Dermer & Böttcher 2006; Dubus 2006; Paredes et al. 2006; Zhang et al. 2009; Takahashi et al. 2009; Yamaguchi & Takahara 2010; Cerutti et al.

2010). They modeled the system in a microquasar scenario (Dermer & Böttcher 2006; Paredes et al. 2006; Zhang et al. 2009; Takahashi et al. 2009), which includes jets from the accreting compact object, or in a colliding wind scenario (Dubus 2006), which includes a relativistic pulsar wind colliding with a stellar wind. In each scenario, they obtained results more or less consistent with the observations for all energy bands.

However, in explaining the X-ray emission as the synchrotron radiation, there is a crucial problem. The magnetic field of around 3 Gauss is required to reproduce the *Suzaku* spectrum (Takahashi et al. 2009; Yamaguchi & Takahara 2010; Cerutti et al. 2010), if the magnetic field is uniform and if a relativistic motion of a radiating medium is neglected. Under this magnetic field the cooling rate of the synchrotron process dominates that of the inverse Compton (IC) process for electrons with $\gtrsim 1$ TeV. This leads to a severe suppression of the flux in TeV range, so that H.E.S.S. spectra cannot be reproduced, as shown in Cerutti et al. (2010).

On the other hand, the work trying to explain X-ray emission as IC process has been limited. Bosch-Ramon et al. (2005) suggested that the X-ray emission was due to the IC (and/or synchrotron) process from the jets and that the orbital variation of the accretion rate was responsible for the X-ray modulation before H.E.S.S. and *Suzaku* observations were reported. After this study, the IC model for the X-ray emission has not been discussed. In the light of the new observational data, we revisit the IC model to reproduce the spectra and the orbital modulation of the X-ray emission. In this paper we aim to find the condition to reproduce the *Suzaku* data when we take the same parameters as in our previous paper, Yamaguchi & Takahara (2010) (hereafter YT10).

We describe the model in Section 2, and show obtained results in Section 3, where we demonstrate that the IC model can well reproduce the X-ray observations if certain conditions are satisfied. We discuss remaining problems and complexities in Section 4.

Finally, we summarize the study in Section 5.

2. IC emission model for X-ray emission

2.1. Model overview

We assume that high energy electrons are accelerated with an isotropic distribution at the position of the compact object. Here, we do not specify the acceleration mechanism, i.e., the microquasar model or the wind collision model. Since the electrons are in the stellar radiation field, they lose energy by IC process. We neglect the synchrotron cooling by assuming that the magnetic energy density is much lower than the radiation energy density. This cooling process leads to modification of the electron distribution as given in the next section. On the other hand, the electrons emit X-rays and gamma rays by scattering off the stellar radiation. Since the stellar radiation field is anisotropic, the high energy emission is also anisotropic resulting from anisotropic IC scattering. This anisotropy affects the modulation of the emission.

Here, we focus on low energy electrons whose IC photons are not subject to $\gamma\gamma$ absorption, which have been neglected in previous works. In YT10, we injected electrons with $3 \times 10^3 < \gamma < 10^8$ and calculated IC scattering, the $\gamma\gamma$ absorption and subsequent cascade process. In addition, we calculated the IC cooling down to $\gamma_e = 3 \times 10^3$. Thus, we focused on the emission from higher energy electrons. Takahashi et al. (2009) also concentrated on high energy IC emission ($\gtrsim 1$ GeV). In this paper we calculate the emission from electrons with lower energy, which emit X-rays and MeV gamma rays through the IC process.

2.2. Electron distribution

The energy distribution of injected electrons $n_{\text{inj}}(\gamma)$ is assumed as

$$n_{\text{inj}}(\gamma) \propto \gamma^{-p} \quad \text{for } \gamma_{\text{min}} < \gamma < \gamma_{\text{max}}, \quad (1)$$

where γ_{min} and γ_{max} are the minimum and maximum Lorentz factors of the injected electrons, respectively. Because gamma rays up to 30 TeV have been detected from LS 5039, we assume $\gamma_{\text{max}} = 10^8$. However, now we are interested in X-ray emission. Moreover, we have calculated GeV to TeV emission due to IC process by the Monte Carlo method and successfully reproduced the observations in YT10. Therefore, in this paper we calculate the IC emission from the electrons with $\gamma < \gamma_1 \equiv 3 \times 10^3$, which corresponds to the minimum Lorentz factor in YT10. In addition, we adopt the same power-law index of the injected electrons as in YT10, i.e., $p = 2.5$, and we assume that p and the coefficient in Equation (1) are constant in the whole orbit.

The electrons severely lose energy due to the strong radiation field by the star. Given the energy density of the stellar radiation, the cooling time by IC process in the Thomson regime is

$$t_{\text{IC,T}} \sim 3 \times 10^4 \gamma^{-1} \left(\frac{a}{a_{\text{peri}}} \right)^2 \text{ s}, \quad (2)$$

where a represents the binary separation and 'peri' means periastron and γ is the Lorentz factor of electrons. Equation (2) implies that injected electrons completely cool near the periastron in $T_{\text{orb}}/10 \sim 3 \times 10^4$ s, where T_{orb} is the orbital period, while at the apastron electrons cool down to $\gamma_c \sim 4$ in $T_{\text{orb}}/10$, where γ_c means the Lorentz factor of cooled electrons.

Therefore, the electron distribution is modified by IC cooling. As a result, if $\gamma_{\text{min}} > \gamma_c$

the distribution in the steady state is given by the following form,

$$n(\gamma) \propto \begin{cases} \gamma^{-2} & \text{for } \gamma_c < \gamma < \gamma_{\min} \\ \gamma^{-(p+1)} & \text{for } \gamma_{\min} < \gamma < \gamma_1 \end{cases}. \quad (3)$$

The normalization of this distribution is determined by equating the number of electrons with γ_1 to that obtained at γ_1 by the Monte Carlo calculation in YT10. Therefore the electron distribution of Equation (3) is continuously joined to that of YT10. We note that $n(\gamma)$ in YT10 is just a boundary condition in this paper, so that the calculation below does not affect so much the GeV spectra. At the same time some mismatches between the model and observed spectra at the GeV band remain.

2.3. Parameter γ_{\min}

We assume that γ_{\min} is a free parameter so that we fit the IC emission spectra from these electrons with the *Suzaku* data. The X-ray flux observed by *Suzaku* anti-correlates with the *Fermi* flux. If we assume that γ_{\min} is constant with the orbital phase, we expect that the fluxes at the two energy bands correlate with each other. This is because the orbital modulation is wholly due to anisotropic IC. In this case, the light curve of *Fermi* is reproduced by the anisotropy of IC process (see YT10), but that of *Suzaku* cannot be reproduced. Therefore, we should assume that γ_{\min} varies with the orbital phase so that the X-ray light curve fits the observed one. We note that this assumption is completely ad hoc at this stage, but it is possible that γ_{\min} varies with the orbital phase because the condition of the electron injection could change with the orbital separation.

Here, we discuss the relation between the X-ray flux and γ_{\min} in order to understand how we should set the variation of γ_{\min} . We define $F_{x,0}$ and $n_0(\gamma_x)$ as the IC X-ray flux and the electron number spectrum at γ_x , respectively, expected when γ_{\min} is constant with

the orbital phase, where γ_x represents the Lorentz factor of electrons emitting X-ray, i.e., $\gamma_x \sim 10$. We note that $F_{x,0}$ shows the orbital modulation similar to the *Fermi* flux F_{GeV} because the modulation of $F_{x,0}$ correlates with that of the IC flux in the GeV band and because this GeV flux well reproduces the *Fermi* flux (see YT10). When γ_{min} varies with the orbital phase, the expected X-ray flux F_x and the electron number spectrum $n(\gamma_x)$ satisfy the relation

$$F_x = F_{x,0} \frac{n(\gamma_x)}{n_0(\gamma_x)}. \quad (4)$$

Using Equation (3), we obtain

$$n(\gamma_x) = n(\gamma_1) \left(\frac{\gamma_{\text{min}}}{\gamma_1} \right)^{-(p+1)} \left(\frac{\gamma_x}{\gamma_{\text{min}}} \right)^{-2}. \quad (5)$$

Since we assume that the electron number at γ_1 varies in the same way as that in YT10, we set

$$n(\gamma_1) = n_0(\gamma_1). \quad (6)$$

When γ_{min} is constant during the whole orbit, $n_0(\gamma_1)$ shows the same modulation as $n_0(\gamma_x)$, so that we obtain

$$n(\gamma_1) \propto n_0(\gamma_x). \quad (7)$$

Therefore, Equation (5) leads to

$$n(\gamma_x) \propto n_0(\gamma_x) \gamma_{\text{min}}^{1-p} \quad (8)$$

As a result, Equation (4) reduces to

$$F_x \propto F_{x,0} \gamma_{\text{min}}^{-1.5}, \quad (9)$$

where we set $p = 2.5$. Therefore, we should increase γ_{min} when $F_{x,0}(F_{\text{GeV}})$ increases and vice versa, in order to reproduce the observed orbital modulation at X-rays.

2.4. Assumptions for the calculation

We assume that the electrons which follow the energy distribution given by Equation (3) are in a steady state for a given orbital phase because $\gamma_x > \gamma_c$. The stellar radiation is assumed to take a black-body distribution. The typical energy is 10 eV, so that IC scattering occurs in the Thomson regime for electrons $\gamma < \gamma_1$. Therefore, we calculate numerically the IC spectra in the Thomson regime, which is done in the same manner as in Dubus et al. (2008). Here, we neglect the effect of secondary electrons created by the cascade process.

3. Calculated Results

In Figure 1, the resultant spectra from low energy electrons (solid lines), the IC spectra from high energy electrons obtained in YT10 (dashed lines) and their sums (thin solid lines) are shown, where the spectra are averaged in the two orbital phases, around the inferior conjunction $\phi = 0.45-0.9$ (red lines and circles) and around the superior conjunction $\phi = 0.9-0.45$ (blue lines and circles). Here, ϕ means the orbital phase, and $\phi = 0$ represents the periastron. The orbital variation of γ_{\min} is given so that the light curve of the observation with *Suzaku* is reproduced (Figure 2). We set the minimum Lorentz factor of cooling electrons as $\gamma_c = 5$, so that the cooling time of electrons with this Lorentz factor is shorter than a tenth of the orbital period at any orbital phase (see Section 2.2). The inclination angle is taken as $i = 30^\circ$ so that this model is consistent with YT10. The orbital parameters are taken from Sarty et al. (2011). The results do not change so much even if we take other allowable parameter sets (e.g. those given in Aragona et al. 2009).

We determine the orbital variation of γ_{\min} by fitting the calculated light curve to the observed one as shown in Figure 2. The comparison of the variation of γ_{\min} with the *Fermi*

light curve is shown in Figure 3, where γ_{\min} is shown with a solid line, $F_{x,0}$ is shown with a dashed line, and the flux obtained with *Fermi* is shown by crosses with dashed error bars. Figure 3 indicates that γ_{\min} obtained from the fitting to the X-ray band shows almost the same variation as the IC flux with the constant injection, that is,

$$\gamma_{\min} \propto F_{x,0} \sim F_{\text{GeV}}. \quad (10)$$

In other words, if we assume the variability of γ_{\min} as Equation (10), we can reproduce the observation with *Suzaku*. The reason why the fitting to the data of *Suzaku* yields such a simple relation is that the observed fluxes of X-ray and GeV bands are related as

$$F_x \propto F_{\text{GeV}}^{-\frac{1}{2}}. \quad (11)$$

In addition to the orbital variation of γ_{\min} , we note that this result gives a lower limit of γ_{\min} . If γ_{\min} is lower than $\sim 10^3$, calculated flux overpredicts the *Suzaku* one.

4. Discussion

We have shown in the previous section that the orbital modulation of the X-ray emission from LS 5039 is reproduced by the IC process if we give the ad hoc relation of Equation (10). However, it is not clear if such a dependence is expected. It is hard to assume that the minimum Lorentz factor of injected electrons varies in tandem with the line of sight. Nevertheless, since the existence of cooled electrons is inevitable, it is natural that the low energy electrons with $\gamma \sim 10$ is responsible for the X-ray emission from LS 5039.

In the model of this paper, the X-ray modulation is mainly due to the variation of the number of cooled electrons. Since the number of cooled electrons is determined by the injection rate $\int n_{\text{inj}}(\gamma)d\gamma$, the X-ray modulation is controlled by the injection rate. In this paper, we assume that p and the coefficient in Equation (1) are constant in the

whole orbit while γ_{\min} modulates. Here we note that the injection rate changes with the orbital motion. That is, the X-ray modulation is adjusted by making γ_{\min} change in this paper. Alternatively, we may adjust the X-ray modulation by changing p and the coefficient because these two parameters are also related to the injection rate.

While the *Suzaku* spectra are well fitted in Figure 1, the calculated spectra in the GeV band match worse the observation since we adopt the YT10 data as higher energy spectra. The *Fermi* spectrum around the superior conjunction is now somewhat overpredicted even for the lowest two bins of *Fermi* spectrum. This means that the amplitude of the modulation in the GeV band is slightly overpredicted when the contribution from low energy electrons is considered. Therefore, in order to reproduce the *Fermi* observation we should set the smaller amplitude of the calculated light curve than the current model, which corresponds to a smaller inclination angle. Smaller inclination angle means a larger mass of the compact object, strengthening the suggestion in YT10 that it is a black hole. This modification of the inclination angle does not affect so much Equation (10) although the amplitude of $F_{x,0}$ and thereby that of γ_{\min} are slightly modified. We note that in this model TeV gamma-ray can be emitted by the IC process since this model is compatible with the model in YT10.

Here, we mention the effect of the escape of electrons on the model. We assume in this paper that electrons cool down to γ_c without escaping. However, when taking into account the hydrodynamics of the system, e.g., the outflow of the jet in the microquasar scenario, if we assume that electrons are advected by the flow, they cannot cool radiatively so efficiently. For example, if electrons are advected at the light speed, the crossing time in the system t_{cross} is ~ 100 s. Since the electrons cool during this crossing time, γ_c is determined by

$$t_{\text{IC,T}} = t_{\text{cross}}, \quad (12)$$

where $t_{\text{IC,T}}$ is given by Equation (2). Thus, we obtain $\gamma_c \sim 300$, which means that electrons do not emit X-rays through the IC scattering if advection is very fast. This issue may be solved in two ways. One is the adiabatic cooling where the spatial extent of electron confinement increases more than two orders of magnitude. The other is that electron injection itself continues to as low as $\gamma_{\text{min}} \sim 10$ with an index 2.0 below a break, then the photon index in the X-ray band may be reproduced. Since $\gamma_c > \gamma_{\text{min}}$, electrons emitting X-rays are not affected by the IC cooling. In these scenarios, the X-ray flux may modulate due to not only the anisotropic IC process but also the orbital variation of γ_c , but further study is required to reproduce the *Suzaku* observations.

We comment shortly models based on the synchrotron emission. If we ascribe the X-ray emission to the synchrotron radiation, the TeV observation cannot be reproduced as shown in Cerutti et al. (2010). This discrepancy may be solved by a model in which the magnetic field is non-uniform. For example, X-rays are emitted in a compact region where the magnetic field is more than 3 Gauss and the electrons are populated in energies lower than 1 TeV, while TeV IC emission by the higher energy electrons takes place in an extended region with magnetic field strength as small as 0.1 Gauss. As an alternative scenario addressing this problem, we could consider a situation where the radiative matter moves along near the line of sight at relativistic velocity. In this scenario, the *Suzaku* spectra would be reproduced under the magnetic field less than 1 Gauss because of the relativistic beaming, and a severe suppression in the TeV band could be avoidable.

Takahashi et al. (2009) proposed the model in which the X-ray emission is explained by the synchrotron radiation. They assume that the adiabatic cooling is more efficient than the radiative cooling, so that the X-ray flux is proportional to the adiabatic cooling time. Thus, the X-ray light curve can be reproduced if one give properly the variation of the adiabatic cooling time. Moreover, since the adiabatic cooling does not change the

power-law index of the electron distribution, the spectral index in the X-ray band is also reproduced if one give $n_{\text{inj}}(\gamma) \propto \gamma^{-2}$. In addition, they show that calculated TeV spectra match the H.E.S.S. observation. The suppression in the TeV band is avoided in this model because high energy electrons cool not radiatively but adiabatically, so that they are not affected by the synchrotron cooling.

Many authors have constructed models in which the parameters of injected electrons vary with the orbital motion to reproduce the observations. Paredes et al. (2006) and Zhang et al. (2009) calculated the emission from the jet in the microquasar scenario and showed broad band spectra from radio to TeV gamma-ray band. Paredes et al. (2006) assumed that the injection rate of the electron distribution varied with the orbital motion due to the change in the accretion rate, and investigated the orbital modulation in each energy band. However, their calculation was based on the data before *Suzaku*. Zhang et al. (2009) assumed that the electron power-law index and the accretion rate, which is equivalent to the injection rate, showed two values for two orbital phase, superior and inferior conjunctions, respectively. As a result, the *Suzaku* spectra are well reproduced but they did not mention the orbital modulation for any energy band. Sierpowska-Bartosik & Torres (2008a) and Sierpowska-Bartosik & Torres (2008b) calculated the IC scattering from electrons in the pulsar wind in the wind collision scenario and showed that their spectra and light curves reproduced the H.E.S.S. data. They assumed that the distribution of the injected electrons showed two different power-law indices for the two phase intervals, respectively, in order to reproduce the H.E.S.S. spectra. However, they have not investigated X-ray emission.

Bednarek (2011) assumed that in the wind collision scenario electrons were accelerated in two shocks separated by a contact discontinuity. He have shown that the IC emission from the pulsar-side shock and the star-side shock accounts for TeV emission and GeV emission, respectively. In his model the maximum energy of electrons varied with the orbital

motion, and the injection rate was constant. As a result, the normalization of the electron distribution is changed, so that X-ray emission by the synchrotron radiation modulates, although the flux varies inversely to the *Suzaku* data.

The crucial difference between the IC model and the synchrotron model is in the MeV spectra. The IC model in this paper predicts that there is no dip in MeV spectra. In contrast, the synchrotron model predicts that there is a dip in MeV spectra (Takahashi et al. (2009), YT10, Cerutti et al. (2010)). Therefore, future observations in the MeV band will judge which model is realized.

5. Summary

We assume that X-ray emission from LS 5039 is due to the IC scattering of electrons with $\gamma \sim 10$. We calculate the anisotropic IC emission from electrons with the Lorentz factor $5 < \gamma < 3 \times 10^3$ in the Thomson regime. As a result, we have found that we can reproduce *Suzaku* flux if the minimum Lorentz factor of injected electrons $\gamma_{\min} \sim 10^3$. Moreover, the X-ray light curve is well reproduced if a simple relation $\gamma_{\min} \propto F_{\text{GeV}}$ is satisfied, where F_{GeV} represents the GeV flux. We have obtained these results based on YT10, where the index and the coefficient of the power-law distribution for injected electrons do not change with respect to the orbital phase. We may obtain different results when we adopt the model in which the index and the coefficient vary, but *Suzaku* data can be reproduced by adjusting these parameters, because the X-ray flux variation is primarily determined by the number of low energy electrons. Thus, we suggest that the X-ray emission obtained with *Suzaku* can be explained by the IC emission. However, we need more investigation for explaining the *Fermi* data. This model will be justified or rejected by future observations in the MeV range.

M.S.Y. is supported by a Grant-in-Aid for JSPS Research Fellowships for Young Scientists (A231860).

REFERENCES

- Abdo, A. A., et al. 2009, *ApJ*, 706, 56
- Aharonian, F., et al. 2005a, *Science*, 309, 746
- Aharonian, F., et al. 2005b, *A&A*, 442, 1
- Aharonian, F., et al. 2006, *A&A*, 460, 743
- Aragona, C., McSwain, M. V., Grundstrom, E. D., et al. 2009, *ApJ*, 698, 514
- Aharonian, F., et al. 2007, *A&A*, 496, L1
- Albert, J., et al. 2006, *Science*, 312, 1771
- Bednarek, W. 2011, *MNRAS*, 418, L49
- Bongiorno, S. D., et al. 2011, *ApJ*, 737, 11
- Bosch-Ramon, V., Paredes, J. M., Ribó, M., Miller, J. M., Reig, P., & Martí, J., 2005, *A&A*, 628, 388
- Casares, J., Ribó, M., Ribas, I., Paredes, J. M., Martí, J., & Herrero, A. 2005, *MNRAS*, 364, 899
- Cerutti, B., Malzac, J., Dubus, G., & Henri, G. 2010, *A&A*, 519, 81
- Dermer, C. D. & Böttcher, M. 2006, *ApJ*, 643, 1081
- Dubus, G. 2006, *A&A*, 456, 801
- Dubus, G., Cerutti, B., & Henri, G. 2008, *A&A*, 477, 691
- Fermi LAT Collaboration et al., 2012, *Science*, 335, 189

Paredes, J. M., Bosch-Ramon, V. & Romero, G. E. 2006, *A&A*, 451, 259

Sarty, G. E., et al. 2011, *MNRAS*, 411, 1293

Sierpowska-Bartosik, A., & Torres, D. F. 2008a, *ApJ*, 674, 89

Sierpowska-Bartosik, A., & Torres, D. F. 2008b, *Astropart. Phys.*, 30, 239

Takahashi, T., et al. 2009, *ApJ*, 697, 592

Yamaguchi, M. S. & Takahara, F. 2010, *ApJ*, 717, 85 (YT10)

Zhang, J.-F., Zhang, L., & Fang, J. 2009, *PASJ*, 61, 949

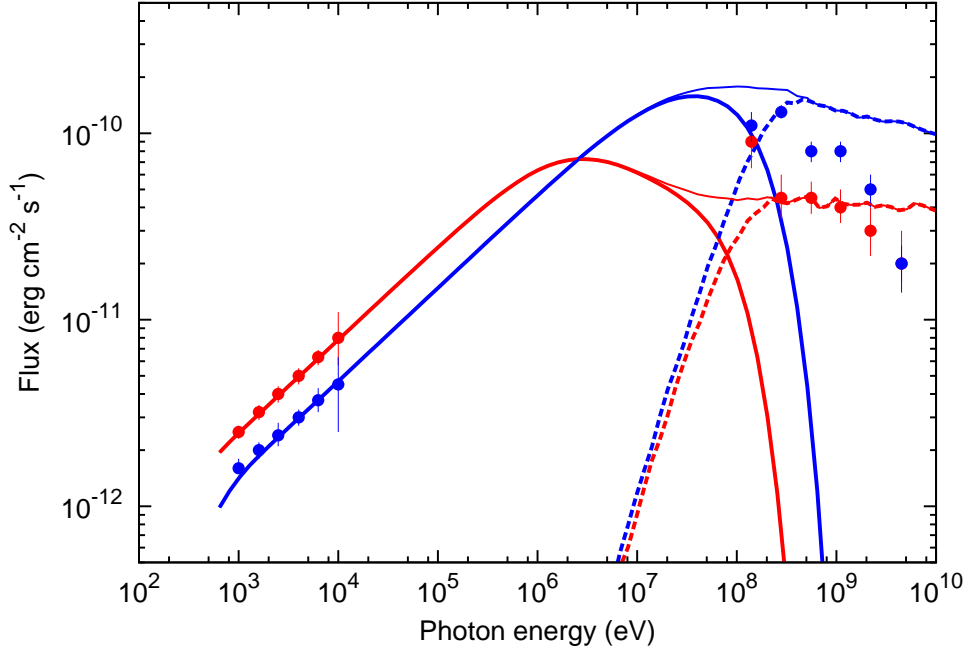


Fig. 1.— IC spectra by low energy electrons ($\gamma < 3 \times 10^3$). The spectra are averaged in the two orbital phases, around inferior conjunction 0.45-0.9 (red lines and circles) and around superior conjunction 0.9-0.45 (blue lines and circles). The observed spectra are shown by circles with error bar for *Suzaku* (XIS, Takahashi et al. 2009) and *Fermi* (Abdo et al. 2009). IC spectra obtained by Monte Carlo method for $\gamma > 3 \times 10^3$ are also shown with dashed curves, which are equivalent to those in Figure 6 of YT10. We change γ_{\min} as a function of the orbital phase (Figure 3) so that the calculated X-ray light curve fits the observed one as shown in Figure 2. Thin solid lines show the sums of the spectra from low and high energy electrons in each phase.

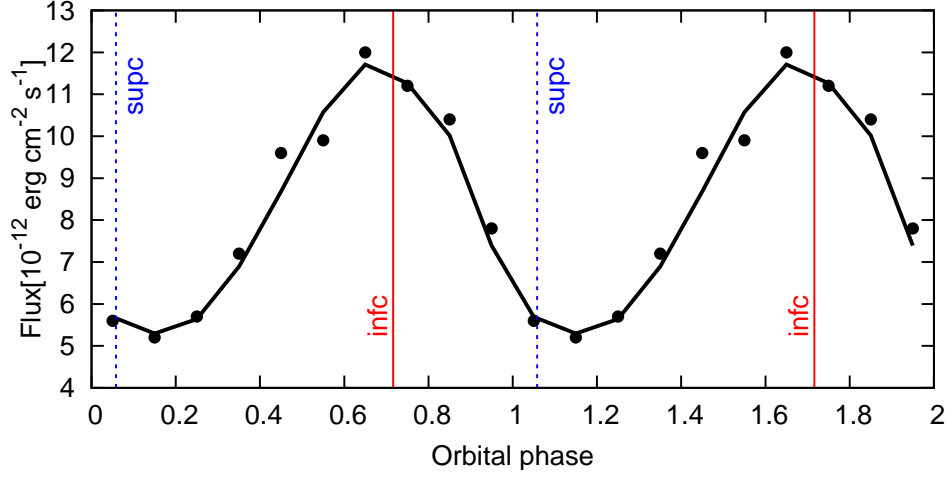


Fig. 2.— Calculated (solid line) and observed (circles) X-ray light curves for the case as in Figure 1. The vertical lines show the superior conjunction (supc) and inferior conjunction (infc).

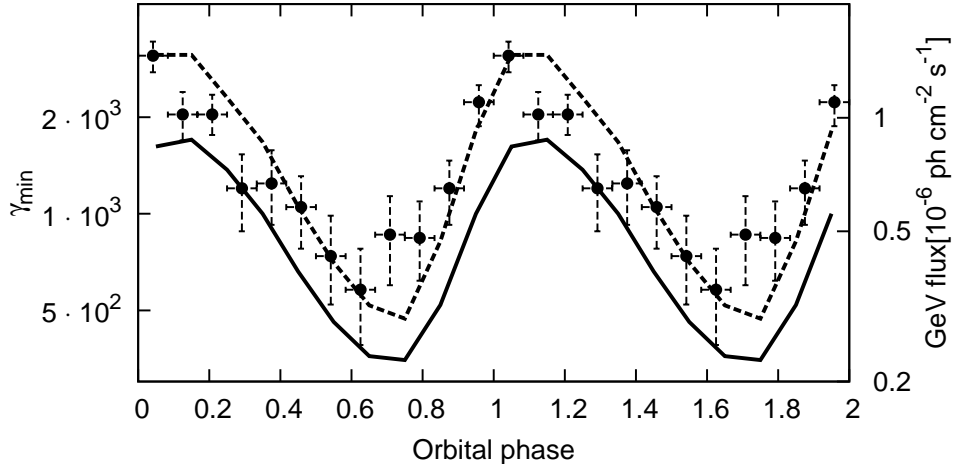


Fig. 3.— Adopted phase dependence of γ_{\min} (solid line) for the case of Figures 1 and 2. Dashed line shows $F_{x,0}$, and circles with dashed error bar show the observed GeV light curve.